Mechanics & Industry **18**, 210 (2017)

DOI: 10.1051/meca/2016030
www.mechanics-industry.org

Mechanics & Industry

MHD flow and heat transfer of Casson nanofluid over a wedge

Macha Madhu[a] and Naikoti Kishan

Department of Mathematics, Osmania University, Hyderabad, Telangana, 500007 India

Received 27 January 2016, Accepted 28 April 2016

Abstract – Heat transfer characteristics of a steady, two dimensional, magnetohydrodynamic boundary layer flow of Casson nanofluid over a wedge have been investigated by incorporating the effects of Brownian motion and thermophoresis. The flux of volume fraction of nanoparticles is taken zero on the boundary. Using suitable similarity transformation, the governing partial differential equations for the modelling of boundary layer flow are reduced to ordinary differential equations. The resulting coupled non-linear ordinary differential equations are successfully solved numerically with the help of variational finite element method. To validate the present analysis the numerical results are compared with previously published work available in the literature and they found to be in good agreement. The effects of the flow controlling parameters on velocity, temperature and nanoparticle volume fraction profiles are investigated. The skin-friction co-efficient, Nusselt number and Sherwood number presented for several set of values of the physical parameters and salient features are analyzed.

Key words: Brownian motion / Casson fluid / FEM / nanofluid / thermophoresis / wedge

1 Introduction

In the recent years, non-Newtonian fluids have become more and more important due to their industrial applications. In fact, the interest in boundary layer flows of non-Newtonian fluid is increasing substantially due to its large number of practical applications in industry, manufacturing processing and biological fluids. Few of main examples related to applications are plastic polymer, drilling mud, optical fibers, paper production, hot rolling, metal spinning and cooling of metallic plates in a cooling bath and many others. Because of several industrial technological applications, the non-Newtonian fluids are considered more important than viscous fluids. Unlike the viscous fluids there is not a single constitutive equation available in the literature by which the behavior of all the non-Newtonian fluids can be analyzed. In fact this is due to the diversity of non-Newtonian fluids in nature. Several rheological models of non-Newtonian fluids have been proposed to represent the viscosity function of these fluids. There are several non-Newtonian models, one among them is the Casson fluid model. Casson fluid model is a simple non-Newtonian fluid model of differential type. In the literature, the Casson fluid model is sometimes stated to fit the rheological data, and it is better than general viscoplastic models for many materials. Casson fluid exhibits a yield stress. If a shear stress less than the yield stress is applied to the fluid, it behaves like a solid whereas if a shear stress greater than the yield stress is applied, it starts to move. The Casson model is more accurate at both very high and very low shear rate. The Casson model has been used in other industries to give a more accurate representation of high shear rate viscosities when only low and intermediate shear rate data are available. Moreover, the Casson fluid has significant applications in polymer processing industries and biomechanics. Casson fluid is a shear thinning liquid that has an infinite viscosity at a zero rate of shear, a yield stress below which no flow occurs, and a zero viscosity at an infinite rate of shear.

As the governing equations of non-Newtonian fluids are highly nonlinear and much more complicated than those of Newtonian fluids, much care is needed in investigating such fluids for the understanding of the flow characteristics of a non-Newtonian fluid. Mathematicians as well as medical researcher are widely working on Casson nanofluid model. Boundary layer flow of Casson fluid over different geometries is considered by many authors in recent years. Nadeem et al. [1] presented MHD flow of a Casson fluid over an exponentially shrinking sheet. Recent contributions on the flow analysis of Casson fluids include Hayat et al.[2], Bhattacharyyaa et al.[3], and Mukhopadhyay et al. [4], Nadeem et al. [5], Haq et al. [6].

The convective flow past a wedge has been extensively studied by many researchers owing to its applications in aerodynamics, geothermal systems, heat exchangers and so forth. Moreover, the wedge flow is important due to

[a] Corresponding author: madhumaccha@gmail.com

the fact that each value of wedge angle yields a different pressure profile, thereby offering insight into boundary layer behavior in number of situation. In 1931, Falkner and Skan studied the similarity solutions of boundary layer flow over a static wedge which is immersed in a viscous fluid. In the last few years, many researchers have investigated Falkner-Skan flow considering different effects. Liu and Chang [7], presented a simple but accurate method to estimate the unknown initial boundary conditions by utilizing the Lie-group shooting method on the Blasius and Falkner-Skan equations. Alizadeh et al. [8] studied the same problem by the Adomian decomposition method, which is a semi analytical method. The Falkner-Skan wedge flow for a non-Newtonian fluid with a variable free stream condition was studied numerically by Postelnicu and Pop [9]. Kafoussias and Nanousis [10] investigated the MHD laminar boundary-layer flow of a non-Newtonian fluid over a permeable wedge. Swati Mukhopadhyay et.al [11] investigated boundary layer forced convection flow of a Casson fluid past a symmetric wedge. Kishan [12, 13] studied MHD heat transfer to non-newtonian power-law fluids flowing over a wedge. Wedge flow problem under various thermophysical conditions was considered by several researchers viz. Hossain et al. [14], Chamkha et al.[15], Pantokratoras [16], Mukhopadhyay [17], Pal and Mondal [18] and others.

Nowadays, the cooling of electronic devices is the major industrial requirement due to the fast technology, but the low thermal conductivity rate of ordinary base fluids includes water, ethylene glycol and oil is the basic limitation. To over come on such limitation, the nanoscale solid particles are submerged into host fluids which change the thermophysical characteristics of these fluids and enhanced the heat transfer rate dramatically. Choi [19] was the first who identified this colloidal suspension. The recent developments in nanofluids and their mathematical modeling, play vital role in industrial and nanotechnology. The nanofluids are used in the applications such as cooling of electronics, heat ex-changer, nuclear reactor safety, hyperthermia, biomedicine, engine cooling, vehicle thermal management and many others. Two mechanisms have been processed to explain the enhancement of the effective thermal conductivity in nanofluids, the first one being the contribution from the higher thermal conductivity of the nanoparticles and second one, the contribution from the Brownian motion of the nanoparticles. The significance of the two contributions is closely related to the bulk temperature of the nanoparticles suspension, the size of the nanoparticles and the volume fraction of the nanoparticles in the nanofluid, as well as the thermo physical properties of the nanoparticles and the base fluid materials.

Non-Newtonian nanofluid is important in many industrial and technological applications such as biological solutions, melts of polymers, paint, tars and glues. Because of this, researches on non-Newtonian fluids have recently become very important. Transport phenomena associated with magnetohydrodynamics arise in physics, geophysics, astrophysics and many branches of chemical engineering which includes crystal magnetic damping control, hydromagnetic chromatography; conducting flow in trickle-bed reactors and enhanced magnetic filtration control. Malik et al. [20] investigated boundary layer flow of Casson nanofluid over a vertical exponentially stretching cylinder. Haq [21] studied heat transfer and MHD effects on Casson nanofluid flow over a shrinking sheet. Madhu and Kishan [22] investigated MHD mixed convection stagnation-point flow of a non-Newtonian power-law nanofluid towards a stretching surface. Mustafa and Khan [23] studied MHD flow of Casson nanofluid past a non-linearly stretching. Ibrahim and Makinde [24] examines the effect of slip and convective boundary condition on magnetohydrodynamic (MHD) stagnation point flow and heat transfer due to Casson nanofluid past a stretching sheet. Using the Buongiorno [25] model, Kuznetsov and Nield [26] studied the influence of nanoparticles on a natural convection boundary layer flow passing a vertical plate. It is interesting to note that the Brownian motion of nanoparticles at molecular and nanoscale levels is a key nanoscale mechanism governing their thermal behaviors. In nanofluid systems, due to the size of the nanoparticles, the Brownian motion takes place, which can affect the heat transfer properties. Brownian motion serves to warm the boundary layer and simultaneously exacerbates particle deposition away from the fluid regime, thereby accounting for the reduced concentration magnitudes.

To the best of authors knowledge, the Casson nanofluid boundary layer flow over a wedge under the influence of magnetic field has not yet addressed in the available literature. Keeping this fact in mind, the present study investigates the flow and heat transfer characteristics for a Casson nanofluid on a wedge under the influence of uniform transverse magnetic field. The effects of the various flow controlling parameters on velocity, temperature and nanoparticle volume fraction have been investigated numerically and analyzed with the help of their graphical representations.

2 Mathematical formulation

Consider a steady, two-dimensional, laminar boundary-layer flow of a non-Newtonian Casson nano fluid past a symmetrical sharp wedge (Fig. 1) and its velocity is given by $u_e(x) = U_\infty \left(\frac{x}{L}\right)^m$ for $m \leqslant 1$ where L is a characteristic length and m is the wedge angle parameter related to the included angle $\pi\beta_1$ by $m = \frac{\beta_1}{2-\beta_1}$. It is worth mentioning that β_1 is a measure of the pressure gradient. If β_1 is positive, the pressure gradient is negative (favorable), and a negative value of β_1 denotes a positive pressure gradient (adverse). For $m < 0$, the solution becomes singular at $x = 0$, while for $m > 0$, the solution can be determined for all values of x. A uniform transverse magnetic field of strength B_0 is applied parallel to the y-axis. It is assumed that the induced magnetic field, the external electric field, and the electric field due to the polarization of charges are negligible. Under these assumptions, the governing

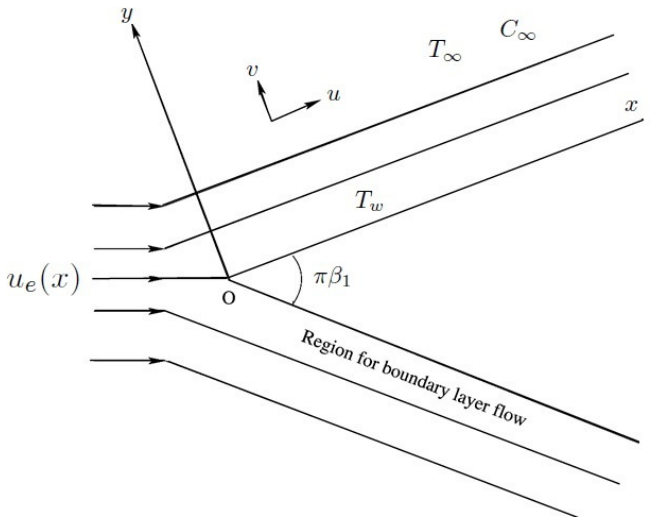

Fig. 1. Flow configuration and co-ordinate system.

equations of the steady, laminar boundary layer flow over a wedge are given by:

$$\frac{\partial u}{\partial x}+\frac{\partial v}{\partial y}=0 \tag{1}$$

$$u\frac{\partial u}{\partial x}+v\frac{\partial u}{\partial y}=u_e\frac{\partial u_e}{\partial x}+\nu\left(1+\frac{1}{\beta}\right)\frac{\partial^2 u}{\partial y^2}-\frac{\sigma}{\rho_f}B_0^2u \tag{2}$$

$$u\frac{\partial T}{\partial x}+v\frac{\partial T}{\partial y}=\alpha\frac{\partial^2 T}{\partial y^2}+\tau\left[D_B\frac{\partial C}{\partial y}\frac{\partial T}{\partial y}+\frac{D_T}{T_\infty}\left(\frac{\partial T}{\partial y}\right)^2\right] \tag{3}$$

$$u\frac{\partial C}{\partial x}+v\frac{\partial C}{\partial y}=D_B\frac{\partial^2 C}{\partial y^2}+\frac{D_T}{T_\infty}\frac{\partial^2 T}{\partial y^2} \tag{4}$$

The associated boundary conditions are

$$u=0,\ v=0,\ T=T_w, D_B\frac{\partial C}{\partial y}+\frac{D_T}{T_\infty}\frac{\partial T}{\partial y}=0,\ \text{at } y=0, \tag{5a}$$

$$u\to u_e(x), T\to T_\infty,\ \ C\to C_\infty \quad \text{at} \quad y\to\infty \tag{5b}$$

where u is the velocity component along x-direction and v is the velocity component along y-direction. Further, ρ_f, σ, υ, B_0, ρ and ρ_p are respectively, the density of the base fluid, electrical conductivity, kinematic viscosity, strength of the magnetic field, density of the fluid and density of the particles. Here, β is the Casson parameter, U_∞ is the main stream velocity and ν is the kinematic viscosity of the fluid. T and C are fluid temperature and nanoparticles fraction, respectively. T_w and T_∞ are the temperature of the fluid at the wall and ambient temperature when $y\to\infty$. C_∞ is the ambient nanoparticle volume fraction when $y\to\infty$. D_B and D_T are respectively, the Brownian diffusion coefficient and thermophoretic diffusion coefficient. $\tau=\frac{(\rho c)_p}{(\rho c)_f}$ is the ratio between the effective heat capacity of the nanoparticles material and heat capacity of the fluid.

Introducing, the following similarity transformations

$$\eta=y\sqrt{\frac{(m+1)U_\infty}{2\nu L^m}}x^{\frac{m-1}{2}}, \psi=\sqrt{\frac{2\nu U_\infty}{(m+1)L^m}}x^{\frac{m+1}{2}}f(\eta),$$
$$\theta(\eta)=\frac{T-T_\infty}{T_w-T_\infty},\ \phi(\eta)=\frac{C-C_\infty}{C_\infty} \tag{6}$$

where ψ is defined as $u=\frac{\partial\psi}{\partial y}$, $v=-\frac{\partial\psi}{\partial x}$. Using Equation (6), automatically satisfy the continuity Equation (1).

In terms of $f(\eta)$, $\theta(\eta)$ and $\phi(\eta)$ Equations (2)–(4) become:

$$\left(1+\frac{1}{\beta}\right)f'''+ff''+\frac{2m}{m+1}\left(1-f'^2\right)-Mf'=0 \tag{7}$$

$$\frac{1}{Pr}\theta''+f\theta'+Nb\theta'\phi'+Nt\theta'^2=0 \tag{8}$$

$$\phi''+Le\ f\ \phi'+\frac{Nt}{Nb}\theta''=0 \tag{9}$$

Using Equation (6), the boundary conditions becomes,

$$f=0,\ \ f'=0,\quad \theta=1,\ \ Nb\phi'+Nt\theta'=0 \quad \text{at} \quad \eta=0 \tag{10a}$$

$$f'\to 1,\ \ \theta\to 0,\ \ \phi\to 0 \quad \text{as} \quad \eta\to\infty \tag{10b}$$

In these expressions $Pr=\frac{\nu}{\alpha}$ is Prandtl number, $M=\frac{\sigma B_0^2}{a\rho}$ is the magnetic field strength parameter, $Nb=\frac{(\rho c)_p D_B C_\infty}{\nu(\rho c)_f}$ represents the Brownian motion, $Nt=\frac{(\rho c)_p D_T(T_w-T_\infty)}{T_\infty\nu(\rho c)_f}$ thermophoresis parameter, $Le=\frac{\upsilon}{D_B}$ the Lewis number.

The physical quantity of major interest is the local skin friction coefficient, local Nusselt number and local Sherwood number in non-dimensional form is given by

$$Re_x^{1/2}C_{f_x}=\left(1+\frac{1}{\beta}\right)f''(0), Re_x^{-1/2}Nu_x$$
$$=-\theta'(0), Re_x^{-1/2}Sh_x=-\phi'(0) \tag{11}$$

Re_x is the local Reynolds number.

3 Method of solution

The finite element method is a powerful technique for solving ordinary or partial differential equations. The steps involved in the finite element analysis are as follows:

- Discretization of the domain into elements.
- Derivation of element equations.
- Assembly of element equations.
- Imposition of boundary conditions.
- Solution of assembled equations.

The whole flow domain is divided into 1000 linear elements of equal size, the element size is taken as $\Delta\eta=0.008$. At each node four functions are to be evaluated;

Table 1. Comparison of Values of $f''(0)$ for Variable Values of m for Newtonian Fluid.

m	Yih [27]	Chamkha et al. [15]	Pal and Mondal [18]	Present results
–0.05	0.213484	0.213802	0.213484	0.213762
0	0.332057	0.332206	0.332206	0.332154
0.33	0.757448	0.757586	0.757586	0.757431
1	1.232588	1.232710	1.232710	1.232705

hence after assembly of all the elemental equations, we obtain a matrix of the order 4004×4004. The obtained system is non-linear, therefore an iterative scheme is utilized in the solution. After imposing the boundary conditions the remaining system contains 3997 equations, which is solved by the Gauss elimination method while maintaining an accuracy of 10^{-5}.

4 Results and discussion

In order to validate the present numerical method, the obtained numerical results are verified with the results obtained by Yih [27], Chamkha et al.[15] and Pal and Mondal [18] for the values of $f''(0)$ in case of newtonian fluid. Thus, it can be seen from Table 1 that the numerical results are in closed agreement with those of previously published works. The influence of physical parameters such as Casson fluid parameter β, wedge angle parameter m, magnetic field parameter M, Brownian motion Nb, thermophoresis parameter Nt, and Lewis number Le, on the magneto hydrodynamic boundary layer flow and heat transfer of Casson nanofluid over a wedge is investigated numerically. In ordered to understand the mathematical model the computational results are presented graphically for velocity, temperature and nanoparticle volume fraction profiles for different values of flow controlling parameters in Figures 2–7. The skin friction co-efficient $(1 + 1/\beta) f''(0)$, Nusselt number $-\theta'(0)$ and Sherwood number $-\phi'(0)$ graphs are presented through Figures 8–11.

Figure 2 illustrates the effect of β on velocity and temperature profiles. Velocity is found to be increasing with Casson fluid parameter β, decreasing nature of the momentum boundary layer thickness is observing with increasing of β. It is noticed from figure that the temperature profiles decrease with the increase of β. Figure 3 exhibit the velocity and temperature profiles for various values of wedge angle parameter m. It is observed that the velocity profiles increase with increasing the wedge angle parameter m, whereas the temperature field decreases with the increase of m. Figures 4a and 4b illustrate the effect of magnetic field parameter M on velocity, temperature and concentration profiles. It is shown that the velocity profiles decreases with the increasing of M, this implies that the momentum boundary layer thickness becomes thinner as M increase. Physically, as M increasing it leads to strong Lorentz force along the vertical direction which offers more resistancy to the flow. It is also observed that the temperature profiles increases with the increasing of magnetic field parameter M. It indicates that the thermal boundary layer thickness increases as M increases. It

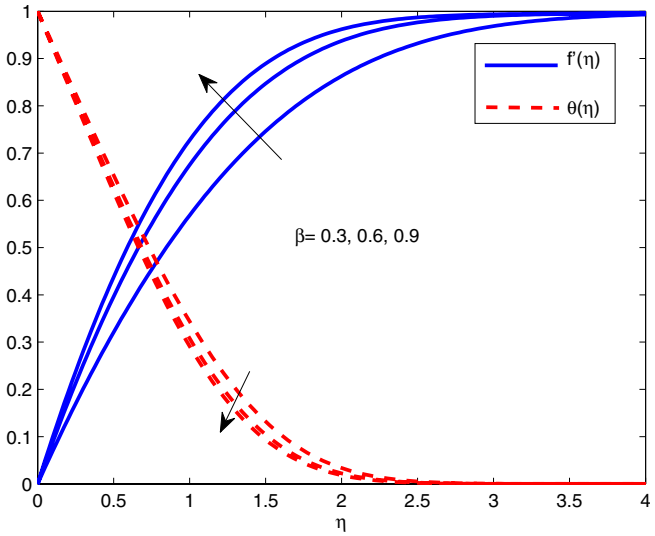

Fig. 2. Effect of β on velocity and temperature profiles.

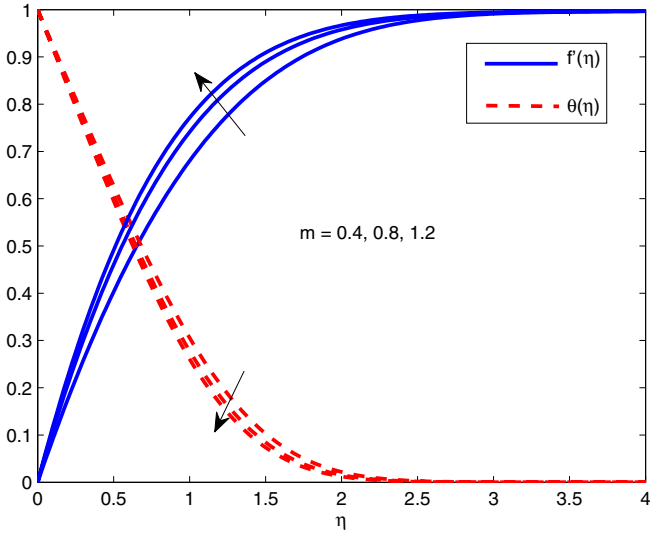

Fig. 3. Effect of m on velocity and temperature profiles.

indicates that the transverse magnetic field opposes the transport phenomena. This is due to the fact that the variation in magnetic field leads to the variation of the Lorentz force produces more resistance to the transport phenomena. From Figure 4b it is seen that the nanoparticle volume fraction profiles increase as M increases.

Figures 5a and 5b present the influence of thermophoresis parameter Nt on the temperature and nanoparticle volume fraction profiles. It is noticed that the temperature is an increasing function of

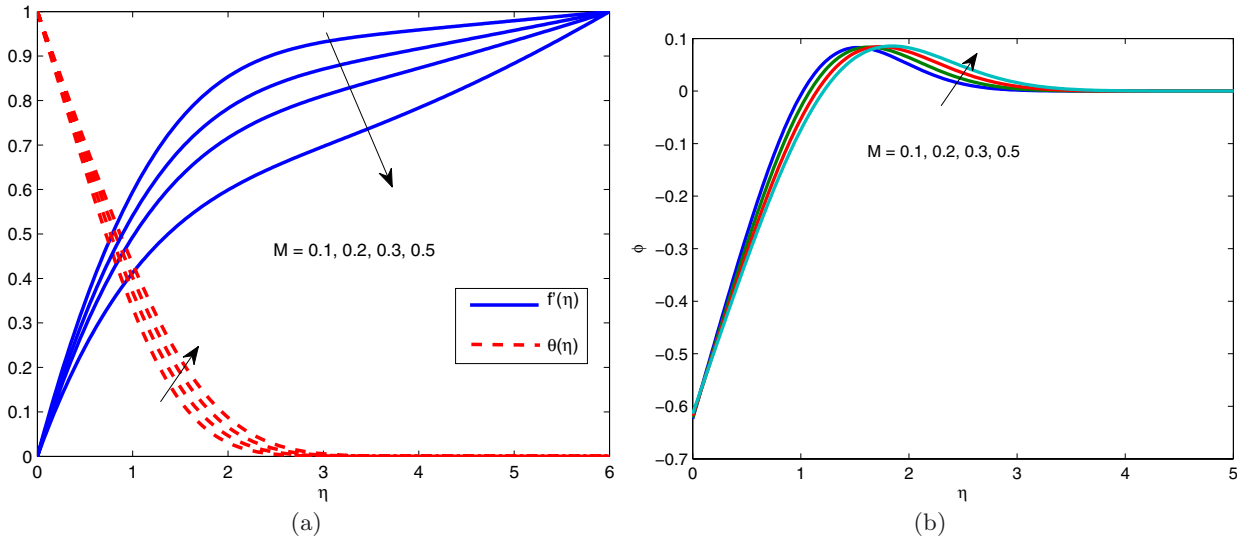

Fig. 4. Effect of M on velocity, temperature and nanoparticle volume fraction profiles.

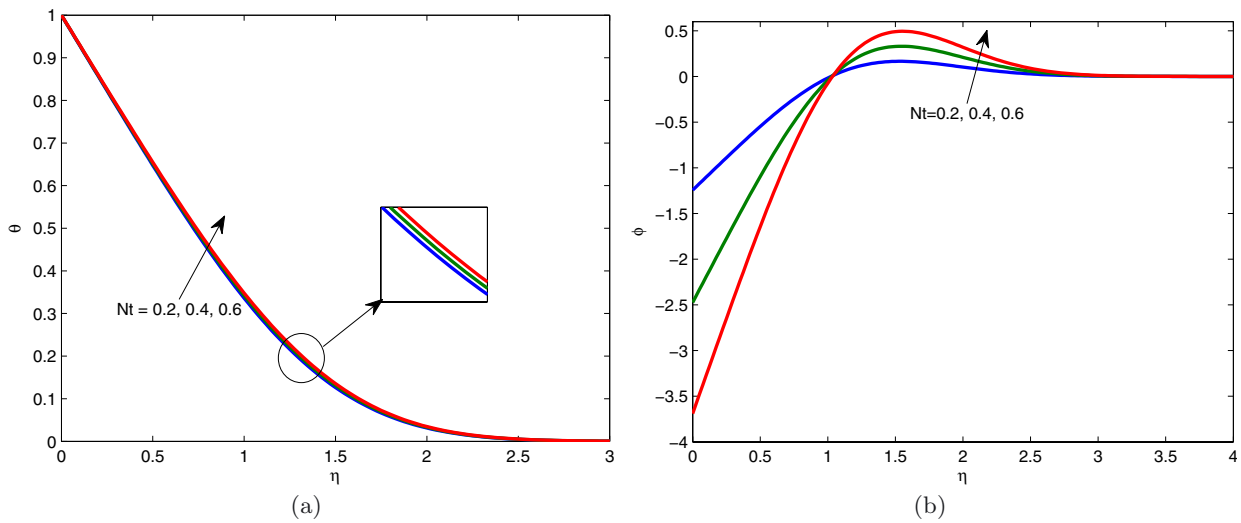

Fig. 5. Effect of Nt on temperature and nanoparticle volume fraction profiles.

thermophoresis Nt. Figure 5b indicate that the thermophoresis Nt is to increases the nanoparticle volume fraction profiles. An intense thermophoretic effect permeates larger extant of fluid with nanoparticles of (higher thermal diffusion) and thus augments the thermal boundary layer thickness. In thermophoretic effect nanoparticle moves away from the hot boundary to towards the cold fluid under the influence of temperature gradient. Figure 6 presents the influence of Brownian motion parameter Nb on nanoparticle volume fraction profiles. The influence of Brownian motion Nb decreases the nanoparticle volume fraction profiles. The effect of Brownian diffusion D_B on the temperature profiles is meger, as also observed by Kuzenotsava and Nield, for brevity it is not shown graphically. The effect of Lewis number can be found from Figure 7. It is noticed that with the increase of Lewis number Le nanoparticle volume fraction profiles decrease. From the definition of Lewis number, a higher value of Lewis number causes a lower Brownian motion coefficient D_B having a kinematic viscosity ν. Due to that, higher Lewis number reduces the nanoparticles volume fraction and its boundary layer thickness.

Figure 8 exhibits the variation of skin-friction co-efficient $(1 + 1/\beta)\, f''(0)$ versus Casson fluid parameter β for different values of m and M. It is very clear that the skin-friction co-efficient is increased with increase of m, whereas it decreases with the effect of magnetic parameter M. It is also seen that as β increases skin-friction co-efficient decreases. Figure 9 gives the plots of Nusselt number $-\theta'(0)$ augments the Casson fluid parameter β for different values of wedge angle parameter m and magnetic field parameter M. It is observed that Nusselt number $-\theta'(0)$ increases with increasing m, whereas it decreases with increasing M. It is evident from figure that $-\theta'(0)$ values increases along with the increasing of β. In Figure 10 the effect of thermophoresis parameter Nt on

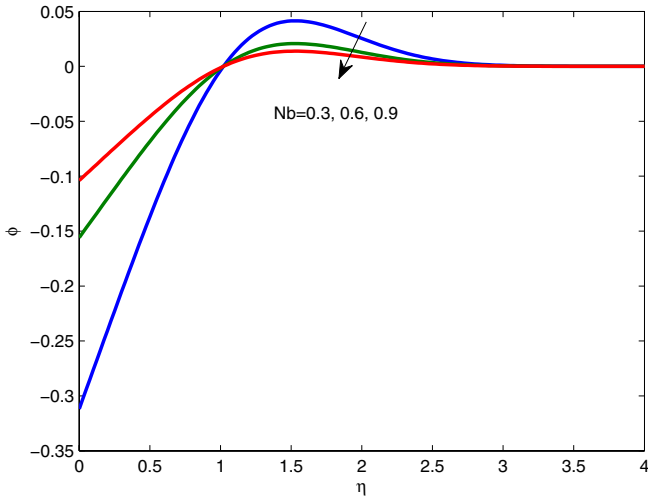

Fig. 6. Effect of Nb on nanoparticle volume fraction profiles.

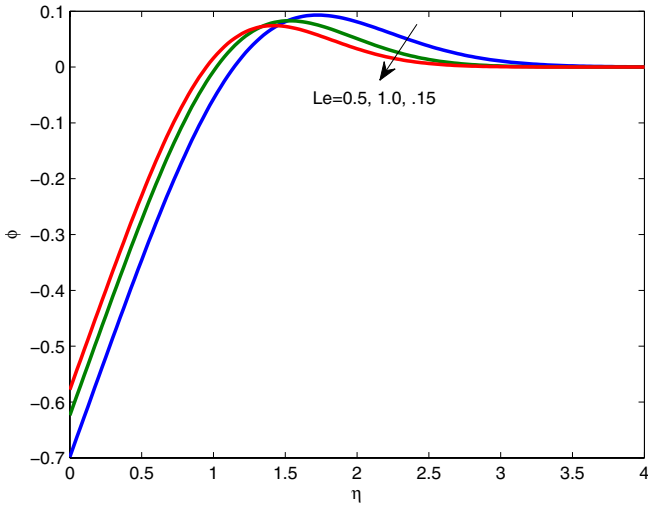

Fig. 7. Effect of Le on nanoparticle volume fraction profiles.

Nusselt number is presented for different values of Lewis number. The Nusselt number decreases significantly with the increasing of thermophoresis parameter Nt as well as Lewis number Le. Figure 11 shows that the diminution in Sherwood number $-\phi'(0)$ occurs when the thermophoretic effect is enhanced. It is also observed that the effect of Brownian motion Nb is to increase the values of Sherwood number.

5 Conclusions

In this work, an analysis has been presented to study the heat transfer characteristics of a study magneto hydrodynamics boundary layer flow of Casson nanofluid over a wedge by incorporating the effects of brownian and thermophoresis. Governing partial differential equations are reduced to ordinary differential equations by using suitable similarity transformations. Based on the results

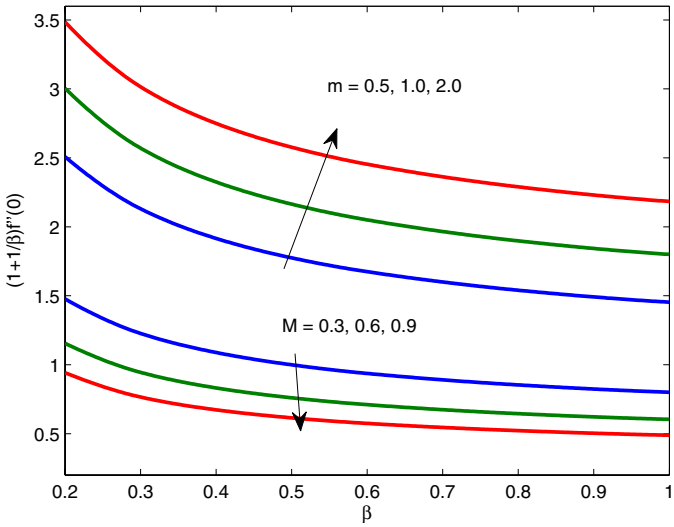

Fig. 8. Effects of β, m and M on skin friction coefficient.

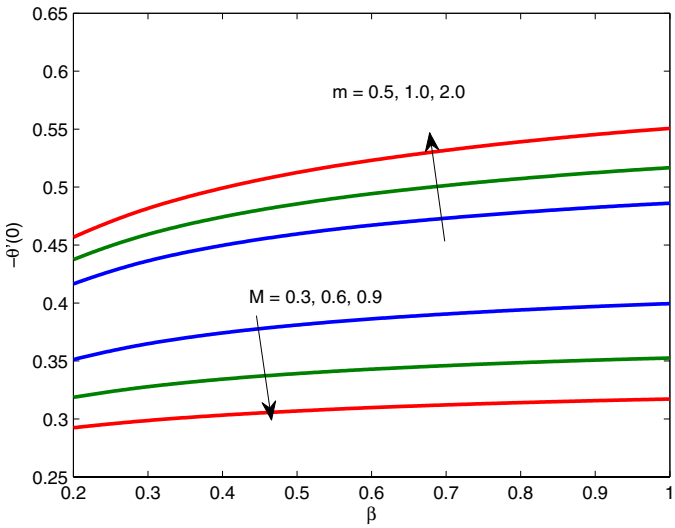

Fig. 9. Variation of heat transfer rate with β, m and M.

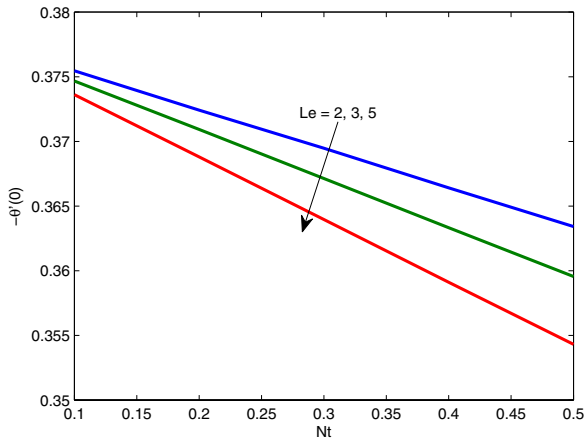

Fig. 10. Effects of Nt and Le on local Nusselt number.

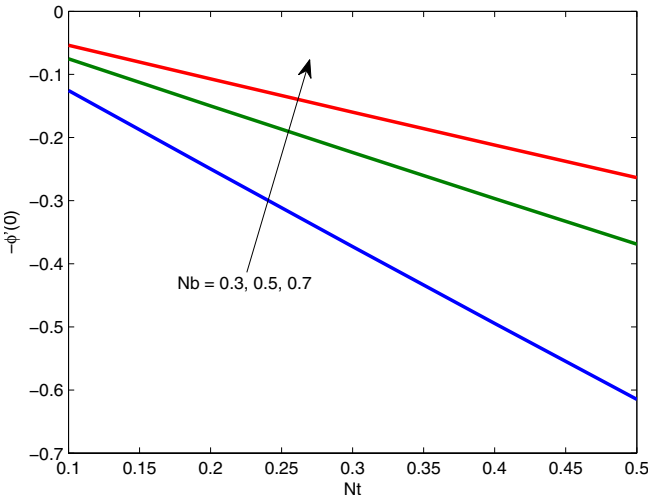

Fig. 11. Effects of Nt and Le on local Sherwood number.

presented above, the following specific conclusions have been drawn:

- The effect of magnetic field parameter M is to reduce the velocity while enhances the temperature and nanoparticle volume fraction profiles.
- The effect of Casson fluid parameter β and wedge angle parameter m enhances the velocity profiles where as reduces the temperature profiles.
- The nanoparticle profiles decrease with the increase of Brownian motion Nb, Lewis number Le where as it they increase with the increase of thermophoresis Nt.
- The skin-friction co-efficient values increase for the increasing value of m while reduce with the increasing value of M and β.
- The rate of heat transfer $-\theta'(0)$ values decrease with the increase of M, Le and Nt where as $\theta'(0)$ values decrease with the increase of β, m.
- The limiting cases of this paper are in good agreement with the result of Yih [27], Chamkha et al. [15] and Pal and Mondal [18].

References

[1] S. Nadeem, R.U. Haq, C. Lee, MHD flow of a Casson fluid over an exponentially shrinking sheet, Sci. Iranica B 19 (2012) 1550–1553

[2] T. Hayat, S.A. Shehzad, A. Alsaedi, Soret and Dufour effects on magnetohydrodynamic (MHD) flow of Casson fluid, Appl. Math. Mech. 33 (2012) 1301–1312

[3] K. Bhattacharyyaa, T. Hayat, A. Alsaedic, Analytic solution for magnetohydrodynamic boundary layer flow of Casson fluid over a stretching/shrinking sheet with wall mass transfer, Chin. Phys. B 22 (2013) 024702

[4] S. Mukhopadhyay, I. Chandra Mondal, A.J. Chamkha, Casson fluid flow and heat transfer past a symmetric wedge, Heat Transfer Asian Res. 42 (2013) 665–675

[5] S. Nadeem, R.U. Haq, N.S. Akbar, MHD three dimensional boundary layer flow of Casson nanofluid past a linearly stretching sheet with convective boundary condition, IEEE Trans. Nonotechnol. 13 (2014) 109–115

[6] R.U. Haq, S. Nadeem, Z.H. Khan, T.G. Okedayo, Convective heat transfer and MHD effects on Casson nanofluod flow over a shrinking sheet, Cent. Eur. J. Phys. 12 (2014) 862–871

[7] C.S. Liu, J.R. Chang, The Lie-group shooting method for multiple-solutions of Falknera Skan equation under suction injection conditions, Int. J. Non-Linear Mech. 43 (2008) 844–851

[8] E. Alizadeh, M. Farhadi, K. Sedighi, H.R. Ebrahimi-Kebria, A. Ghafourian, Solution of the Falkner-Skan equation for wedge by Adomian Decomposition Method, Commun. Nonlinear Sci. Numer. Simul. 14 (2009) 724–733

[9] A. Postelnicu, I. Pop, Falkner-Skan boundary layer flow of a power-law fluid past a stretching wedge, Appl. Math. Comput. 217 (2011) 4359–4368

[10] N.G. Kafoussias, N.D. Nanousis, Magnetohydrodynamic laminar boundary-layer flow over a wedge with suction or injection, Can. J. Phys. 75 (1997) 733–745

[11] S. Mukhopadhyay, I. Chandra Mandal, Boundary layer flow and heat transfer of a Casson fluid past a symmetric porous wedge with surface heat flux, Chin. Phys. B 23 (2014) 4

[12] N. Kishan, P. Kavitha, Quasi linearization approach to MHD heat transfer to non-newtonian power-law fluids flowing over a wedge with heat source/sink in the presence of viscous dissipation, IJMCAR. 3 (2013) 15–28

[13] N. Kishan, P. Amrutha, MHD heat transfer to non-Newtonian power-law fluids flowing over a wedge with viscous dissipation, IJAME 14 (2009) 965–987

[14] M.A. Hossain, M.S. Munir, D.A.S. Rees, Flow of viscous incompressible fluid with temperature dependent viscosity and thermal conductivity past a permeable wedge with uniform surface heat flux, Int. J. Therm. Sci. 39 (2000) 635–644

[15] A.J. Chamkha, M.M. Quadri, I. Camille, Thermal radiation effects on MHD forced convection flow adjacent to a non-isothermal wedge in the presence of a heat source or sink, Heat Mass Transf 39 (2003) 305–312

[16] A. Pantokratoras, The Falkner-Skan flow with constant wall temperature and variable viscosity, Int. J. Therm. Sci. 45 (2006) 378–389

[17] S. Mukhopadhyay, Effects of radiation and variable fluid viscosity on flow and heat transfer along a symmetric wedge, J. Appl. Fluid. Mech. 2 (2009) 29–34

[18] D. Pal, H. Mondal, Influence of temperature-dependent viscosity and thermal radiation on MHD forced convection over a nonisothermal wedge, Appl. Math. Comput. 212 (2009) 194–208

[19] S.U.S. Choi, Enhancing Thermal Conductivity of Fluids with Nanoparticles, ASME, USA (1995) 99-105, FED231/MD

[20] M.Y. Malik, M. Naseer, S. Nadeem, A. Rehman, The boundary layer flow of Casson nanofluid over a vertical exponentially stretching cylinder, Appl. Nanosci. 4 (2014) 869–873

[21] Rizwan U.l. Haq, S. Nadeem, Z. Hayyat Khan, Toyin Gideon Okedayo, Convective heat transfer and MHD effects on Casson nanofluid flow over a shrinking sheet, Cent. Eur. J. Phys. 12 (2014) 862–871

[22] M. Madhu, N. Kishan, Magnetohydrodynamic Mixed Convection Stagnation-Point Flow of a Power-Law Non-Newtonian Nanofluid towards a Stretching Surface with Radiation and Heat Source/Sink, J. Fluids 2015 (2015) ID634186

[23] M. Mustafa, J.A. Khan, Model for flow of Casson nanofluid past a non-linearly stretching sheet considering magnetic field effects, AIP Adv. 5 (2015) 077148

[24] W. Ibrahim, O.D. Makinde, Magnetohydrodynamic Stagnation Point Flow and Heat Transfer of Casson Nanofluid Past a Stretching Sheet with Slip and Convective Boundary Condition, J. Aerospace Eng. 29 (2015) 04015037

[25] J. Buongiorno, Convective transport in nanofluids, ASME J. Heat Transfer 128 (2006) 240–250

[26] A.V. Kuznetsov, D.A. Nield, Natural convective boundary-layer flow of a nanofluid past a vertical plate: A revised model, Int. J. Theor. Sci. 77 (2014) 126–129

[27] Yih KA. Forced convection flow adjacent to a non-isothermal wedge, Int. Commun. Heat Mass Transf. 26 (1996) 819–827